International Journal of Analysis and Applications

Mathematical Analysis for the Behavior of the *HIV* Dynamics in a Periodic Environment

Sana Abdulkream Alharbi[1], **Nada A. Almuallem**[2,*]

[1]*Department of Mathematics & Statistics, College of Science, Taibah University, Yanbu 41911, Saudi Arabia*

[2]*Department of Mathematics and Statistics, Faculty of Science, University of Jeddah, P.O. Box 80327, Jeddah 21589, Saudi Arabia*

[*]*Corresponding author:* naalmouallim@uj.edu.sa

Abstract. In this paper, we propose and study an HIV dynamics model that considers three ways of infection, as well as general transmission and neutralization rates in a periodic environment. The model accounts for both latently and productively infected cells. General nonlinear functions are given for the incident rates of infection and the neutralization rates of infected cells and viruses. The basic infection reproduction number, which is the spectral radius of an integral operator, determines the model's global dynamics. We have analyzed the model's asymptotic stability as the value of the basic reproduction number approaches unity. The numerical simulations carried out across three different scenarios support the findings of the theoretical investigation.

1. Introduction

Infectious diseases continue to debilitate and cause inconvenience in humans and animals from the invasion and growth of germs in the body. Several studies were performed to describe, formulate, control, and predict the spread of infectious diseases (see [1–5] and the references therein). Pathogens, which can spread in communities of people, plants, or animals, are what cause infectious diseases. Some of the infectious diseases are transmitted through direct contact with infectious individuals. These diseases are classified into two main categories: Directly transmitted diseases (tuberculosis, *HIV/AIDS*, hepatitis, etc.) and vector-borne diseases such as malaria, yellow fever, dengue fever, and chikungunya. In the global complex biological situation, more and more attention is being paid over time to fundamental specialized studies about infectious diseases such

Received: Dec. 25, 2024.

2020 *Mathematics Subject Classification.* 34C11, 34C12, 34C25, 34C45, 34C60, 37C75, 92-10, 92D30.

Key words and phrases. asymptotic behavior *HIV* dynamics; three infection routes; periodic environment; asymptotic behavior; periodic comportment; uniform persistence.

https://doi.org/10.28924/2291-8639-23-2025-46
ISSN: 2291-8639

as *HIV* and *HBV*. One of the most threatening viral agents is the *HIV*. *HIV* slowly destroys the immune system until *AIDS* develops. Since the discovery of the existence of *HIV* reservoirs, it has become apparent that the majority of pro-viruses were detected in $CD4^{+}T$ lymphocytes with a memory phenotype, i.e. in cells that have previously been activated by an antigen [6]. Following the activation of a naive T lymphocyte by a major histocompatibility complex associated with a peptide, it proliferates rapidly, acquiring effector functions necessary for the elimination of the antigen. When the antigen disappears, the majority of these cells die (contraction phase) and a small number of memory cells persist. This population of memory $CD4^{+}T$ lymphocytes is made up of several sub-populations with significant functional differences and which differ in their ability to persist throughout life [7, 8]. Thus, studies aimed at identifying reservoir cells have rapidly evolved in their level of sophistication in line with discoveries made in fundamental immunology. To date, memory $CD4^{+}T$ cells are generally classified into three sub-populations (stem, central, and effector memory cells). Although these three sub-populations are generally considered the majority reservoirs for *HIV*, naïve $CD4^{+}T$ cells may also play a role in viral persistence.

Mathematical modeling of infectious diseases has become an important tool for public health decision-makers because these models make it possible predict and control the evolution of these diseases. Several models have been formulated for diseases such as malaria, *HIV*/*AIDS*, yellow fever, dengue fever, and tuberculosis, to name but a few (see [5, 9–12] and the references therein). The most proposed mathematical models used nonlinear ordinary-differential equations. Several *HIV* mathematical models have been proposed and studied [13–18], Measles [19,20], and Zika [21, 22]. In particular, the mathematical modeling for *HIV*-1 infection has attracted the interest of several researchers. Most of them focus on the interaction between *HIV*-1 and $CD4^{+}T$ cells, which play the role of the main driver of the immune response. Mathematical models have played an essential role in explaining the behavior of the *HIV* transmission. They are also advantageous to understand and control the AIDS progression. Therefore, the mathematical modeling for the *HIV* transmission is essential to understand the dynamics of the *HIV* free virions as well as the target cells. In [23], the authors proposed the primary *HIV* dynamical system considering three components which are the healthy and infected cells and free virions (*HIV* particles). Several mathematical models [24–29] lead with mathematical modeling of *HIV* dynamics by focusing on the characterization of the interactions of *HIV* with T-lymphocytes. At this time, no medication can eradicate *HIV* from the human body. Substances that have been developed to inhibit various phases of HIV multiplication or to lessen the virus's capacity to infect new CD4 lymphocytes are the drugs utilized to combat the virus. We refer to these medications as "antiviral" or "antiretroviral". Periodic presumed treatments involve administering drugs at predetermined intervals. To maximize benefits, patients should take the drugs daily at the same time, either before or with food. Periodic treatment doses have a consistent impact on patients. As a result, it is critical to consider periodicity when developing a mathematical model. Several studies have looked at the periodicity in mathematical models for different infectious diseases [30–40]. To improve the mathematical model for HIV transmission suggested in [41], we will add the general rates of transmission and neutralization in a periodic setting and add a new section for the variation of B cells.

The rest of this paper is organized as follows: In Section 2, we describe the model and look how HIV dynamics change over time by looking at three ways of infection and their general transmission rates and neutralization rates in a regular setting. First, we will give some basic properties of the model. The basic infection reproduction number denoted as $\mathcal{R}_0$, is defined as the spectral radius of an integral operator. It plays a crucial role in determining the global dynamics of the model. Subsequently, it has been demonstrated that the HIV-free periodic trajectory is globally asymptotically stable when $\mathcal{R}_0 < 1$ and that the virus persists when $\mathcal{R}_0 > 1$ with periodic behavior. Several numerical examples are given in section 3 validating the acquired findings. We conclude with a discussion in section 4 that affirms the results obtained.

2. Epidemic Model Formulation

This compartmental epidemic model is a more generalized version of the ones examined in [41]. It includes a new compartment for B cells variation, as well as the general rates of transmission and neutralization. Here, the total cells are separated into three mutually-exclusive compartments: S, I_l, I_p, These represent the number of cells revealed to be susceptible, latently infected, and productively infected, respectively. We denote by V, W, and T_l to be the number of free HIV particles, B cells, and T lymphocytes, respectively. The infected cells are divided into two compartments based on the condition of the infected cell, specifically I_l or I_p. The incidence rates are given by $\lambda_1 f_1(V)S$, $\lambda_2 f_2(I_l)S$ and $\lambda_3 f_3(I_p)S$ due to the three possible routes of infection. The neutralization function of the productively infected cells is given by $f_4(I_p)$ and the neutralization function of viruses is given by $f_5(V)$.

$$\begin{cases} \dot{I}_l(t) = [\lambda_1(t)f_1(V(t)) + \lambda_2(t)f_2(I_l(t)) + \lambda_3(t)f_3(I_p(t))]S(t) - (\kappa_1(t) + m_l(t))I_l(t), \\ \dot{I}_p(t) = \kappa_1(t)I_l(t) - m_p(t)I_p(t) - \lambda_4(t)f_4(I_p(t))T_l(t), \\ \dot{V}(t) = \kappa_2(t)I_p(t) - m_v(t)V(t) - \lambda_5(t)f_5(V(t))W(t), \\ \dot{S}(t) = m_s(t)S_i(t) - m_s(t)S(t) - [\lambda_1(t)f_1(V(t)) + \lambda_2(t)f_2(I_l(t)) + \lambda_3(t)f_3(I_p(t))]S(t), \\ \dot{W}(t) = \kappa_3(t)V(t) - m_w(t)W(t), \\ \dot{T}_l(t) = \kappa_4(t)I_p(t) - m_c(t)T_l(t) - \lambda_6(t)f_6(I_p(t))T_l(t), \end{cases} \tag{2.1}$$

with initial condition $(I_l^0, I_p^0, V^0, S^0, W^0, T_l^0) \in \mathbb{R}_+^6$.
The model's parameters are positive functions where the significance is resumed in Table 1. The incidence rates $f_1(V)$, $f_2(I_l)$ and $f_3(I_p)$, the productively infected cells neutralization rate $f_4(I_p)$, the viruses neutralization rate $f_5(V)$ and the T-Lymphocytes impairment rate $f_6(I_p)$ are continuous increasing functions equal zero at the origin. Thus, we impose some assumptions on the functions $f_1(V)$, $f_2(I_l)$, $f_3(I_p)$, $f_4(I_p)$, $f_5(V)$ and $f_6(I_p)$. We assume that the parameters of the dynamics, which should be nonnegative, are T-periodic, continuous, and bounded functions. We also assume that the mortality rate of a cell is contingent upon its status.

Symbol	Meaning
I_l	Latently infected cells
I_p	Productively infected cells
V	HIV-1 particles
S	Susceptible cells
W	B cells
T_l	T-Lymphocytes
$f_1(V)$	Infection transmission by V
$f_2(I_l)$	Infection transmission by I_l
$f_3(I_p)$	Infection transmission by I_p
$f_4(I_p)$	Neutralization function of I_p
$f_5(V)$	Neutralization function of viruses V
$f_6(I_p)$	T-Lymphocytes impairment function
λ_1	Contact rate between S and V
λ_2	Contact rate of S and I_l
λ_3	Contact rate of S and I_p
λ_4	Periodic neutralization rate of I_p
λ_5	Periodic neutralization rate of W
λ_6	Periodic T-Lymphocyte impairment contact
m_l	Death rate of I_l
m_p	Death rate of I_p
m_v	Death rate of V
m_s	Death rate of S
m_w	Death rate of B cells, W
m_c	Death rate of T_l
κ_1	Periodic conversion rate from the I_l to I_p
κ_2	Periodic generation rate of HIV particles
κ_3	Periodic recruited rate of B cells, W
κ_4	Periodic T-Lymphocyte immune rate
S_i	Periodic generation rate of susceptible cells

Table 1. Meaning of the model's notations.

Assumption 2.1.

- *f_i, $i = 1, \cdots, 6$ are continuous increasing functions such that $f_i(0) = 0$, for $i = 1, \cdots, 6$.*
- *$\lambda_1(t)$, $\lambda_2(t)$, $\lambda_3(t)$, $\lambda_4(t)$, $\lambda_5(t)$, $\lambda_6(t)$, $m_s(t)$, $m_l(t)$, $m_p(t)$, $m_v(t)$, $m_w(t)$, $m_c(t)$, $\kappa_1(t)$, $\kappa_2(t)$, $\kappa_3(t)$, $\kappa_4(t)$ and $S_i(t)$ are T-periodic, continuous, and bounded functions.*
- *$m_s(t) \leq m_l(t) \leq m_i(t)$, $\forall\ t \in \mathbb{R}_+$.*

Let us consider $D(t)$ to be a $m\times m$ matrix function that is continuous, T-periodic, irreducible, and cooperative. Hence, $\sigma_D(t)$ denotes to the solution of the equation below

$$\dot{\sigma}(t) = D(t)\sigma(t), \tag{2.2}$$

and by $r(\sigma_D(T))$ the spectral radius of $\sigma_D(T)$ having positive components. The application of the famous theorem of Perron-Frobenius [42] enables us to deduce that $\sigma_D(T)$ has a principal eigenvalue equal to $r(\sigma_D(T))$. Consequently, the following lemma was deduced, which will be useful for the

Lemma 2.1. *(Zhang and Zhao [43, Lemma 2.1].) The equation (2.2) admits a unique solution given by* $\sigma(t) = x(t)e^{\ell t}$ *where* $\ell = \dfrac{1}{T}\ln(r(\sigma_C(T)))$ *such that the function* $x(t)$ *is non-negative and* T*-periodic.*

The equation

$$\dot{S}(t) = m_s(t)(S_i(t) - S(t)), \tag{2.3}$$

with initial condition $S^0 \in \mathbb{R}_+$ admits a unique T-periodic solution denoted by $S^*(t)$ that it is globally attractive in $\mathbb{R}_+$, i.e. $S^*(t) > 0$ for all positive t. Then, the model (2.1) admits a unique virus-free periodic solution given by $Q_0(t) = (0,0,0,S^*(t),0,0)$.

For each continuous, non-negative T-periodic function denoted by $\eta(t)$, let us define $\eta^u = \max_{t\in[0,T)} \eta(t)$ and $\eta^l = \min_{t\in[0,T)} \eta(t)$ and let $m(t) = \min_{t\geq 0}(m_v(t), m_c(t))$. Define $\eta^u = \max_{t\in[0,T)} \eta(t)$ and $\eta^l = \min_{t\in[0,T)} \eta(t)$ for each non-negative T-periodic function $\eta(t)$. Then, let $m(t) = \min_{t\geq 0}(m_v(t), m_c(t))$. Consequently, The model (2.1) is defined within the attractive and bounded set Ω^u as the following.

Proposition 2.1.

$$\Omega^u = \left\{(I_l, I_p, V, S, W, T_l) \in \mathbb{R}^6_+ \ / \ I_l + I_p + S \leq S^u_i; V + T_l \leq (\kappa^u_2 + \kappa^u_4)\frac{S^u_i}{m^l}; W \leq (\kappa^u_2 + \kappa^u_4)\frac{S^u_i \kappa^u_3}{m^l m^l_w}\right\}$$

According to the model (2.1)*,* Ω^u *is a bounded, invariant, and attractor set of any dynamics solution. Moreover, the model (2.1) satisfies*

$$\lim_{t\to\infty} I_l(t) + I_p(t) + S(t) - S^*(t) = 0. \tag{2.4}$$

Proof. By merging the first three equations of the model (2.1), it can be inferred that

$$\begin{aligned}
\dot{I}_l(t) + \dot{I}_p(t) + \dot{S}(t) &= -m_l(t)I_l(t) - m_p(t)I_p(t) - \kappa_1(t)I_l(t) + m_s(t)S_i(t) - m_s(t)S(t) \\
&\quad -\lambda_4(t)f_4(I_p(t))T_l(t) \\
&\leq m_s(t)\Big(S_i(t) - (I_l(t) + I_p(t) + S(t))\Big) \\
&\leq 0, \text{ if } (I_l(t) + I_p(t) + S(t)) \geq S^u_i,
\end{aligned}$$

$$\begin{aligned}\dot{V}(t)+\dot{T}_l(t) &= (\kappa_2(t)+\kappa_4(t))I_p(t)-m_v(t)V(t)-m_c(t)T_l(t)-\lambda_6(t)f_6(I_p(t))T_l(t)\\ &\leq (\kappa_2(t)+\kappa_4(t))I_p(t)-m_v(t)V(t)-m_c(t)T_l(t)\\ &\leq (\kappa_2^u+\kappa_4^u)S_i^u-m(t)(V(t)+T_l(t))\\ &\leq 0,\ \text{if}\ m(t)(V(t)+T_l(t))\geq(\kappa_2^u+\kappa_4^u)S_i^u,\end{aligned}$$

and

$$\begin{aligned}\dot{W}(t) &= \kappa_3(t)V(t)-m_w(t)W(t)\\ &\leq (\kappa_2^u+\kappa_4^u)\frac{S_i^u\kappa_3^u}{m^l}-m_w(t)W(t)\\ &\leq 0,\ \text{if}\ W(t)\geq(\kappa_2^u+\kappa_4^u)\frac{S_i^u\kappa_3^u}{m^l m_w^l}.\end{aligned}$$

□

In the following subsection 2.1, we will establish the basic reproduction number $\mathcal{R}_0$ utilizing the theoretical framework introduced in [36]. Later, we will prove that once $\mathcal{R}_0<1$. Consequently, the *HIV*-free periodic trajectory $\mathcal{Q}_0(t)=(0,0,0,S^*(t),0,0)$ is globally asymptotically stable, leading to the disappearance of *HIV*. In the subsection 2.2, we aim to prove that if $\mathcal{R}_0>1$, then the model (2.1) will be uniformly persistent which implies that the virus will persist.

2.1. ***HIV*-free periodic trajectory.** Initially, we seek to establish the definition of the basic reproduction number $\mathcal{R}_0$ and confirm that the assumptions (A1)–(A7) outlined in [36] hold true. Let

$$Z(t)=\begin{pmatrix}I_l(t)\\ I_p(t)\\ V(t)\\ S(t)\\ W(t)\\ T_l(t)\end{pmatrix},\mathcal{P}(t,Z(t))=\begin{pmatrix}(\lambda_1(t)f_1(V(t))+\lambda_2(t)f_2(I_l(t))+\lambda_3(t)f_3(I_p(t)))S(t)\\ \kappa_1(t)I_l(t)\\ \kappa_2(t)I_p(t)\\ 0\\ 0\\ 0\end{pmatrix},$$

$$\Lambda^-(t,Z(t))=\begin{pmatrix}(\kappa_1(t)+m_l(t))I_l(t)\\ m_p(t)I_p(t)+\lambda_4(t)f_4(I_p(t))T_l(t)\\ m_v(t)V(t)\\ (m_s(t)+\lambda_1(t)f_1(V(t))+\lambda_2(t)f_2(I_l(t))+\lambda_3(t)f_3(I_p(t)))S(t)\\ m_w(t)W(t)\\ m_c(t)T_l(t)+\lambda_6(t)f_6(I_p(t))T_l(t)\end{pmatrix},$$

and $\Lambda^+(t,Z(t))=\begin{pmatrix}0\\ 0\\ 0\\ m_s(t)S_i(t)\\ \kappa_3(t)V(t)\\ \kappa_4(t)I_p(t)\end{pmatrix}$. The model (2.1) admits the new form as follows

$$\dot{Z}(t)=\mathcal{P}(t,Z(t))-\Lambda(t,Z(t))=\mathcal{P}(t,Z(t))-\Lambda^-(t,Z(t))+\Lambda^+(t,Z(t)). \tag{2.5}$$

It is easily to see that the satisfaction of Assumptions (A1)–(A5) occurs. Still to prove the satisfaction of Assumptions (A6) and (A7).

The model (2.5) admits an *HIV*-free periodic trajectory, $Z^*(t) = (0,0,0,S^*(t),0,0)^T$.

Let us define the functions $h(t,Z(t)) = \mathcal{P}(t,Z(t)) - \Lambda^-(t,Z(t)) + \Lambda^+(t,Z(t))$ and

$$M(t) = \left(\frac{\partial h_i(t,Z^*(t))}{\partial Z_j}\right)_{4\le i,j\le 6}$$

where $h_i(t,Z(t))$ and $Z_i(t)$ are the i-th component of the functions $h(t,Z(t))$ and $Z(t)$, respectively. It is easy to obtain that

$$M(t) = \begin{pmatrix} -m_s(t) & 0 & 0 \\ 0 & -m_w(t) & 0 \\ 0 & 0 & -m_c(t) \end{pmatrix},$$

with $r(\sigma_M(T)) < 1$. Therefore, the *HIV*-free trajectory $Z^*(t)$ is asymptotically stable inside the set Ω_s defined as follows:

$$\Omega_s = \left\{(0,0,0,S,0,0) \in R^6_+\right\}.$$

Therefore, the sixth condition (A6) of [36] occurs.

Let us define the 3 by 3 matrices $\mathbf{P}(t)$ and $\mathbf{\Lambda}(t)$ given by $\mathbf{P}(t) = \left(\dfrac{\partial \mathcal{P}_i(t,Z^*(t))}{\partial Z_j}\right)_{1\le i,j\le 3}$ and $\mathbf{\Lambda}(t) = \left(\dfrac{\partial \Lambda_i(t,Z^*(t))}{\partial Z_j}\right)_{1\le i,j\le 3}$ where $\mathcal{P}_j(t,Z(t))$ and $\Lambda_j(t,Z(t))$ are the j-th component of $\mathcal{P}(t,Z(t))$ and $\Lambda(t,Z(t))$, respectively. We can easily obtain that

$$\mathbf{P}(t) = \begin{pmatrix} \lambda_2(t)f_2'(0)S^*(t) & \lambda_3(t)f_3'(0)S^*(t) & \lambda_1(t)f_1'(0)S^*(t) \\ \kappa_1(t) & 0 & 0 \\ 0 & \kappa_2(t) & 0 \end{pmatrix}$$

and

$$\mathbf{\Lambda}(t) = \begin{pmatrix} \kappa_1(t) + m_l(t) & 0 & 0 \\ 0 & m_p(t) & 0 \\ 0 & 0 & m_v(t) \end{pmatrix}.$$

By considering the following equation $\dfrac{d}{dt}Y(s_1,s_2) = -\mathbf{\Lambda}(s_1)Y(s_1,s_2)$ with $s_1 \ge s_2$ and $Y(s_1,s_1) = I$, we denote by $Y(s_1,s_2)$ its solution. Therefore, the seventh condition (A7) of [36] occurs.

Let us now define the Banach space of T-periodic functions $\mathbb{R} \mapsto \mathbb{R}^3$, equipped with the norm $||.||_\infty$ and the linear operator $\mathbb{F} : C_T \to C_T$ expressed as follows:

$$(\mathbb{F}\mu)(\nu) = \int_0^\infty Y(\nu,\nu-t)\mathbf{P}(\nu-t)\mu(\nu-t)dt, \ \forall \nu \in \mathbb{R}, \mu \in C_T. \tag{2.6}$$

The definition of the basic reproduction number, $\mathcal{R}_0$ of the model (2.1) is given through the spectral radius of $\mathbb{F}$, and is expressed as follows,

$$\mathcal{R}_0 = r(\mathbb{F}).$$

This definition will help us in studying the stability of the *HIV*-free periodic solution $Q_0(t) = (0,0,0,S^*(t),0,0)$ of system (2.1) in this subsection.

Theorem 2.1. *[36, Theorem 2.2]*

- $\mathcal{R}_0 < 1 \;\Leftrightarrow\; r(\sigma_{\mathbf{P}-\mathbf{\Lambda}}(T)) < 1.$
- $\mathcal{R}_0 = 1 \;\Leftrightarrow\; r(\sigma_{\mathbf{P}-\mathbf{\Lambda}}(T)) = 1.$
- $\mathcal{R}_0 > 1 \;\Leftrightarrow\; r(\sigma_{\mathbf{P}-\mathbf{\Lambda}}(T)) > 1.$

Therefore, the *HIV*-free trajectory $Q_0(t)$ is locally asymptotically stable only once $\mathcal{R}_0 < 1$.

Theorem 2.2. *$Q_0(t)$ is globally asymptotically stable only once $\mathcal{R}_0 < 1$.*

Proof. By using results of Theorem 2.1, $Q_0(t)$ is locally asymptotically stable only if $\mathcal{R}_0 < 1$. Still to prove that $Q_0(t)$ is globally attractive for the case where $\mathcal{R}_0 < 1$. Using the results (2.4) given in Proposition 2.1, for all $\varsigma_1 > 0$, there exists a constant $T_1 > 0$ such that $I_l(t) + I_p(t) + S(t) \le S^*(t) + \varsigma_1$ for $t > T_1$. Then, $S(t) \le S^*(t) + \varsigma_1$, and we get

$$\begin{cases} \dot{I}_l(t) \le [\lambda_1(t)f_1(V(t)) + \lambda_2(t)f_2(I_l(t)) + \lambda_3(t)f_3(I_p(t))](S^*(t)+\varsigma_1) - (\kappa_1(t)+m_l(t))I_l(t), \\ \dot{I}_p(t) = \kappa_1(t)I_l(t) - m_p(t)I_p(t) - \lambda_4(t)f_4(I_p(t))T_l(t), \\ \dot{V}(t) \le \kappa_2(t)I_p(t) - m_v(t)V(t), \end{cases} \tag{2.7}$$

for $t > T_1$. Consider the matrix $M_2(t)$ given by:

$$M_2(t) = \begin{pmatrix} \lambda_2(t)f_2'(0) & \lambda_3(t)f_3'(0) & \lambda_1(t)f_1'(0) \\ 0 & 0 & 0 \\ 0 & 0 & 0 \end{pmatrix}. \tag{2.8}$$

By applying Theorem 2.1, one has $r(\sigma_{\mathbf{P}-\mathbf{\Lambda}}(T)) < 1$ and we choose $\varsigma_1 > 0$ small enough satisfying $r(\sigma_{\mathbf{P}-\mathbf{\Lambda}+\varsigma_1 M_2}(T)) < 1$. Now consider the three-dimensional model as follows

$$\begin{cases} \dot{Y}_l(t) = [\lambda_1(t)f_1(\bar{V}(t)) + \lambda_2(t)f_2(\bar{I}_l(t)) + \lambda_3(t)f_3(\bar{I}_p(t))](S^*(t)+\varsigma_1) - (\kappa_1(t)+m_l(t))\bar{I}_l(t), \\ \dot{Y}_i(t) = \kappa_1(t)I_l(t) - m_p(t)\bar{I}_p(t) - \lambda_4(t)f_4(\bar{I}_p(t))\bar{T}_l(t), \\ \dot{Y}_v(t) = \kappa_2(t)\bar{I}_p(t) - m_v(t)\bar{V}(t). \end{cases} \tag{2.9}$$

By applying Lemma 2.1 and the comparison principle, we obtain the existence of a T-periodic positive function $y_1(t)$ such that

$$x(t) \le y_1(t)e^{k_1 t}$$

with $x(t) = \big(I_l(t), I_p(t), V(t)\big)$ and $k_1 = \dfrac{1}{T}\ln\left(r(\sigma_{\mathbf{P}-\mathbf{\Lambda}+\varsigma_1 M_2}(T)\right) < 0$. Thus, $\lim_{t\to\infty} I_l(t) = \lim_{t\to\infty} I_p(t) = \lim_{t\to\infty} V(t) = 0$. Hence, we obtain $\lim_{t\to\infty} W(t) = \lim_{t\to\infty} T_l(t) = 0$. Furthermore, we have $\lim_{t\to\infty}(S(t) - S^*(t)) = 0$. It can be deduced that the *HIV*-free trajectory $Q_0(t)$ is globally attractive. □

2.2. ***HIV*-Infected Periodic Solution .** Now, we assume that $\mathcal{R}_0 > 1$. We start by considering the Poincaré function $P_f : \mathbb{R}^6_+ \to \mathbb{R}^6_+$ associated to the model (2.1) with $X_0 \mapsto f(T, X^0)$ such that $f(t, X^0)$ is the unique solution of (2.1) where the initial value $f(0, X^0) = X^0 \in \mathbb{R}^6_+$. Let us define the sets Ω, Ω_0, and $\partial\Omega_0$ as follows: $\Omega = \left\{(I_l, I_p, V, S, W, T_l) \in \mathbb{R}^6_+\right\}$, $\Omega_0 = Int(\mathbb{R}^6_+)$ and $\partial\Omega_0 = \Omega \setminus \Omega_0$.

It easy to see that Ω and Ω_0 are positively invariant according to Proposition 2.1 and P_f is point dissipative. Consider the set P_∂ defined as follows

$$P_\partial = \left\{(I_l^0, I_p^0, V^0, S^0, W^0, T_l^0) \in \partial\Omega_0 : P_f^n(I_l^0, I_p^0, V^0, S^0, W^0, T_l^0) \in \partial\Omega_0,\ \forall\, n \geq 0\right\}.$$

In the first step, we need to demonstrate that

$$P_\partial = \{(0, 0, 0, S, 0, 0),\ S \geq 0\}. \tag{2.10}$$

to be able to apply the uniform persistence theory given in [43, 44]. Note that it is evident that $P_\partial \supseteq \{(0, 0, 0, S, 0, 0),\ S \geq 0\}$. Now, in order to prove that $P_\partial \setminus \{(0, 0, 0, S, 0, 0),\ S \geq 0\} = \emptyset$, let $(I_l^0, I_p^0, V^0, S^0, W^0, T_l^0) \in P_\partial \setminus \{(0, 0, 0, S, 0, 0),\ S \geq 0\}$.
Assume that $I_p^0 = 0$ and that $0 < I_l^0$, then for any $t > 0$, $I_l(t) > 0$ and we have $\dot{I}_p(t)_{|t=0} = \kappa_1(0)I_l^0 > 0$. Now, $\forall t > 0$ if $I_p^0 > 0$ and $I_l^0 = 0$, then $I_p(t) \geq 0$ and $S(t) > 0$. Then, for any $t > 0$, we have

$$I_l(t) = \left[I_l^0 + \int_0^t [\lambda_1(\omega)f_1(V(\omega)) + \lambda_2(\omega)f_2(I_l(\omega)) + \lambda_3(\omega)f_3(I_p(\omega))]S(\omega) \times e^{\int_0^\omega (\kappa_1(s) + m_l(s))ds} d\omega\right] e^{-\int_0^t (\kappa_1(s) + m_l(s))ds} > 0,\ \ \forall t > 0.$$

We deduce that $(I_l(t), I_p(t), V(t), S(t), W(t), T_l(t)) \notin \partial\Omega_0$ for very small $0 < t$. By using Proposition 2.1, the set Ω_0 is positively invariant then we deduce (2.10). Consequently, The existence and uniqueness of a fixed point $(0, 0, 0, S^*(0), 0, 0)$ of P_f in P_∂ is established, indicating the persistence of the *HIV* disease.

Theorem 2.3. *Assuming that $\mathcal{R}_0 > 1$ only. There is at least a unique positive periodic trajectory of the model* (2.1) *such that $\exists\, \epsilon > 0$ satisfying $\forall\ (I_l^0, I_p^0, V^0, S^0, W^0, T_l^0) \in Int(R^3_+) \times R_+ \times Int(R^2_+)$,*

$$\liminf_{t\to\infty} I_p(t) \geq \epsilon > 0.$$

Proof. In the beginning, we will show that P_f is uniformly persistent (also the solution of model (2.1)) for $(\Omega_0, \partial\Omega_0)$ ([44],Theorem 3.1.1). By using the results of Theorem 2.1, we obtain $r(\sigma_{\mathbf{P}-\mathbf{\Lambda}}(T)) > 1$ and then $\exists\ \zeta_2 > 0$ sufficiently small satisfying $r(\sigma_{\mathbf{P}-\mathbf{\Lambda}-\zeta_2 M_2}(T)) > 1$. We consider the perturbed dynamics

$$\dot{S}_\beta(t) \;=\; m_s(t)S_i(t) - m_s(t)S_\beta(t) - [\lambda_1(t)f_1(\beta) + \lambda_2(t)f_2(\beta) + \lambda_3(t)f_3(\beta)]S_\beta(t), \tag{2.11}$$

P_f associated with (2.11) has a unique fixed point that it is globally attractive in $\mathbb{R}_+$ denoted here by $\bar{S}^0_\beta$. Applying the implicit function theorem, $\beta \mapsto \bar{S}^0_\beta$ is continuous. Assume that $\beta > 0$ small enough such that $\bar{S}_\beta(t) > \bar{S}(t) - \zeta_2,\ \ \forall\ t > 0$. Let $Q_1 = (0, 0, 0, \bar{S}^0, 0, 0)$. Concerning the initial condition, the solution is continuous and then then $\exists\ \beta^*$ satisfying $\forall\ (I_l^0, I_p^0, V^0, S^0, W^0, T_l^0) \in \Omega_0$ with $\|(I_l^0, I_p^0, V^0, S^0, W^0, T_l^0) - Q_1\| \le \beta^*$, and then

$$\|f(t,(I_l^0, I_p^0, V^0, S^0, W^0, T_l^0)) - f(t,Q_1)\| < \beta,\ \forall\ 0 \le t \le T.$$

Now, we aim to prove that

$$\limsup_{i\to\infty}\ d(P_f^i(I_l^0, I_p^0, V^0, S^0, W^0, T_l^0), Q_1) \ge \beta^* \text{ for any } (I_l^0, I_p^0, V^0, S^0, W^0, T_l^0) \in \Omega_0. \tag{2.12}$$

Assume that it is false, i.e.

$$\limsup_{n\to\infty} d(P_f^i(I_l^0, I_p^0, V^0, S^0, W^0, T_l^0), Q_1) < \beta^*$$

for any $(I_l^0, I_p^0, V^0, S^0, W^0, T_l^0) \in \Omega_0$.
In particular, assume that $\forall i > 0$, $d(P_f^i(I_l^0, I_p^0, V^0, S^0, W^0, T_l^0), Q_1) < \beta^*$. Therefore,

$$\|w(t, P_f^i(I_l^0, I_p^0, V^0, S^0, W^0, T_l^0)) - f(t,Q_1)\| < \beta \text{ for any } i > 0, 0 \le t \le T.$$

Suppose that $t = iT + t_1,\ \forall\ \ t \ge 0$, where $t_1 \in [0,T)$ and $i \le \dfrac{t}{T}$ describe the greatest integer value of $\dfrac{t}{T}$. This implies that

$$\begin{aligned}\|f(t,(I_l^0, I_p^0, V^0, S^0, W^0, T_l^0)) - f(t,Q_1)\| &= \|w(t_1, P_f^i(I_l^0, I_p^0, V^0, S^0, W^0, T_l^0)) - f(t_1,Q_1)\| \\ &< \beta, \qquad\qquad \forall\ t \ge 0.\end{aligned}$$

Let $(I_l(t), I_p(t), V(t), S(t), W(t), T_l(t)) = f(t,(I_l^0, I_p^0, V^0, S^0, W^0, T_l^0))$. Then $0 \le I_l(t), I_p(t)$ and $V(t) \le \beta$ for any $t \ge 0$. Furthermore, we have

$$\dot S(t) \ \ \ge\ \ m_s(t)S_i(t) - m_s(t)S(t) - (\lambda_1(t)f_1(\beta) + \lambda_2(t)f_2(\beta) + \lambda_3(t)f_3(\beta))S(t). \tag{2.13}$$

P_f associated with the new system (2.11) admits $\bar S_\beta^0$ as a fixed point which is globally attractive and satisfying $\bar S_\beta(t) > \bar S(t) - \zeta_2$, therefore, there exists a constant $T_2 > 0$ satisfying

$$\bar S(t) > \bar S(t) - \zeta_2,\ \forall\ t > T_2.$$

Then, for any $t > T_2$

$$\begin{cases} \dot I_l(t) & \ge & [\lambda_1(t)f_1(V(t)) + \lambda_2(t)f_2(I_l(t)) + \lambda_3(t)f_3(I_p(t))](\bar S(t) - \zeta_2) - (\kappa_1(t) + m_l(t))I_l(t), \\ \dot I_p(t) & = & \kappa_1(t)I_l(t) - m_p(t)I_p(t) - \lambda_4(t)f_4(I_p(t))T_l(t), \\ \dot V(t) & = & \kappa_2(t)I_p(t) - m_v(t)V(t) - \lambda_5(t)f_5(V(t))W(t). \end{cases} \tag{2.14}$$

$r(\sigma_{\mathbf{P}-\mathbf{\Lambda}-\zeta_2 M_2}(T)) > 1$, then by using the comparison principle associated with the results of Lemma 2.1, we deduce the existence of T-periodic positive trajectory $y_2(t)$ satisfying $J(t) \ge e^{k_2 t}y_2(t)$ and $k_2 = \dfrac{1}{T}\ln\ r\left(\sigma_{\mathbf{P}-\mathbf{\Lambda}-\zeta_2 M_2}(T)\right) > 0$. Therefore $\lim_{t\to\infty} I_p(t) = \infty$ which is impossible because the trajectory is bounded and then (2.12) is verified. Therefore, P_f is weakly uniformly persistent respecting to $(\Omega_0, \partial\Omega_0)$ and admits a global attractor. Thus, the set $Q_1 = (0,0,0,\bar S^0,0,0)$ is invariant inside Ω and $W^s(Q_1) \cap \Omega_0 = \emptyset$. Therefore, the solutions in P_∂ converge to Q_1 and Q_1 is acyclic in P_∂. By using [44, Theorem 1.3.1 and Remark 1.3.1], we deduce that P_f associated to

$(\Omega_0, \partial\Omega_0)$ is uniformly persistent. Furthermore, according to [44, Theorem 1.3.6], P_f admits a fixed point $(\tilde{I}_l^0, \tilde{I}_p^0, \tilde{V}^0, \tilde{S}^0, \tilde{W}^0, \tilde{T}_l^0) \in \Omega_0$. Moreover, $(\tilde{I}_l^0, \tilde{I}_p^0, \tilde{V}^0, \tilde{S}^0, \tilde{W}^0, \tilde{T}_l^0) \in Int(R_+^3) \times R_+ \times Int(R_+^2)$. Let's prove that $\tilde{S}^0 > 0$. Assume that it is false, i.e. $\tilde{S}^0 = 0$. From the fourth equation of the model (2.1), we have

$$\dot{\tilde{S}}(t) \geq m_s(t)S_i(t) - m_s(t)\tilde{S}(t) - (\lambda_1(t)f_1(\tilde{V}(t)) + \lambda_2(t)f_2(\tilde{I}_l(t)) + \lambda_3(t)f_3(\tilde{I}_p(t)))\tilde{S}(t),$$

such that $\tilde{S}^0 = \tilde{S}(pT) = 0, p = 1, 2, 3, \cdots$. Regarding Proposition 2.1, we can conclude that $\forall\ \varsigma_3 > 0$, there exists $T_3 > 0$ large enough satisfying

$$\tilde{I}_l(t), \tilde{I}_p(t) \leq S_i^u + \varsigma_3, \tilde{V}(t) \leq (\kappa_2^u + \kappa_4^u)\frac{S_i^u}{m^l} + \varsigma_3, t > T_3.$$

Then, we deduce that

$$\begin{aligned}\dot{\tilde{S}}(t) \quad &\geq \quad m_s(t)S_i(t) - m_s(t)\tilde{S}(t) - (\lambda_1(t)f_1(((\kappa_2^u + \kappa_4^u)\frac{S_i^u}{m^l} + \varsigma_3)) + \lambda_2(t)f_2((S_i^u + \varsigma_3)) \\ &+ \quad \lambda_3(t)f_3((S_i^u + \varsigma_3)))\tilde{S}(t)\end{aligned}$$

for any $t \geq T_3$. There exists a constant $\bar{p}$ sufficiently large such that for any $p > \bar{p}$, the inequality $pT > T_3$ holds. Therefore, by applying the comparison principle, we obtain

$$\begin{aligned}\tilde{S}(pT) \quad &= \quad e^{-\int_0^{pT}([\lambda_1(u)f_1((\kappa_2^u + \kappa_4^u)\frac{S_i^u}{m^l} + \varsigma_3) + \lambda_2(u)f_2(S_i + \varsigma_3) + \lambda_3(u)f_3(S_i + \varsigma_3)] + m_s(u))du} \\ &\times \quad \Bigg[\tilde{S}^0 + \int_0^{pT} m_s(\omega)S_i(\omega) \\ &\times \quad e^{\int_0^{\omega}\left([\lambda_1(u)f_1((\kappa_2^u + \kappa_4^u)\frac{S_i^u}{m^l} + \varsigma_3) + \lambda_2(u)f_2(S_i + \varsigma_3) + \lambda_3(u)f_3(S_i + \varsigma_3)] + m_s(u)\right)du} d\omega\Bigg].\end{aligned}$$

Hence, for any $p > \bar{p}$ it is impossible that $S(pT) > 0$. Then $\tilde{S}^0$ should be nonnegative and the solution $(\tilde{I}_l^0, \tilde{I}_p^0, \tilde{V}^0, \tilde{S}^0, \tilde{W}^0, \tilde{T}_l^0)$ of model (2.1) is a positive T-periodic trajectory. □

3. Numerical Examples

Our goal in this section is to perform the theoretical findings concerning the system (2.1) by some numerical examples. We will model all incidence and neutralization rates using some of Holling's type II functions.

$$f_i(x) = \frac{f_i^{max}x}{\zeta_i + x}$$

where f_i^{max} and ζ_i, $i = 1, \cdots, 6$ are nonnegative constants. Note that f_i, $i = 1, \cdots, 6$ are continuous and increasing functions. However, for the model parameters, we will used the seasonally forced function of the form $c(t) = c_0(1 + c_1\cos(n\pi(t + \theta)))$, where $n \in \mathbb{N}$, $c_0 \geq 0$, $0 < c_1 \leq 1$, and $0 \leq \theta \leq 1$ is the phase angle. Therefore, we define the model parameters as follows.

$$\begin{cases} \lambda_1(t) & = & \lambda_{10}(1+\lambda_{11}\cos(n\pi(t+\theta))), & m_s(t) & = & m_{s0}(1+m_{s1}\cos(n\pi(t+\theta))), \\ \lambda_2(t) & = & \lambda_{20}(1+\lambda_{21}\cos(n\pi(t+\theta))), & m_l(t) & = & m_{l0}(1+m_{l1}\cos(n\pi(t+\theta))), \\ \lambda_3(t) & = & \lambda_{30}(1+\lambda_{31}\cos(n\pi(t+\theta))), & m_p(t) & = & m_{i0}(1+m_{i1}\cos(n\pi(t+\theta))), \\ \lambda_4(t) & = & \lambda_{40}(1+\lambda_{41}\cos(n\pi(t+\theta))), & m_v(t) & = & m_{v0}(1+m_{v1}\cos(n\pi(t+\theta))), \\ \lambda_5(t) & = & \lambda_{50}(1+\lambda_{51}\cos(n\pi(t+\theta))), & m_w(t) & = & m_{w0}(1+m_{w1}\cos(n\pi(t+\theta))), \\ \lambda_6(t) & = & \lambda_{50}(1+\lambda_{51}\cos(n\pi(t+\theta))), & m_c(t) & = & m_{c0}(1+m_{c1}\cos(n\pi(t+\theta))), \\ \kappa_1(t) & = & \kappa_{10}(1+\kappa_{11}\cos(n\pi(t+\theta))), & \kappa_2(t) & = & \kappa_{20}(1+\kappa_{21}\cos(n\pi(t+\theta))), \\ \kappa_3(t) & = & \kappa_{30}(1+\kappa_{31}\cos(n\pi(t+\theta))), & \kappa_4(t) & = & \kappa_{40}(1+\kappa_{41}\cos(n\pi(t+\theta))), \\ S_i(t) & = & S_{i0}(1+S_{i1}\cos(n\pi(t+\theta))). & & & \end{cases} \tag{3.1}$$

The seasonal cycles frequencies λ_{11}, λ_{21}, λ_{31}, λ_{41}, λ_{51}, m_{s1}, m_{l1}, m_{i1}, m_{v1}, m_{w1}, m_{c1}, κ_{11}, κ_{21}, κ_{41}, κ_{51}, and S_{i1} are the amplitudes satisfying $|\lambda_{11}| < 1$, $|\lambda_{21}| < 1$, $|\lambda_{31}| < 1$, $|\lambda_{41}| < 1$, $|m_{s1}| < 1$, $|m_{l1}| < 1$, $|m_{i1}| < 1$, $|m_{v1}| < 1$, $|m_{w1}| < 1$, $|m_{c1}| < 1$, $|\lambda_{51}| < 1$, $|\lambda_{61}| < 1$, $|\kappa_{11}| < 1$, $|\kappa_{21}| < 1$, $|\kappa_{31}| < 1$, $|\kappa_{41}| < 1$, and $|S_{i1}| < 1$. The constants λ_{10}, λ_{20}, λ_{30}, λ_{40}, λ_{50}, λ_{60}, m_{s0}, m_{l0}, m_{i0}, m_{v0}, m_{w0}, m_{c0}, κ_{10}, κ_{20}, κ_{30}, κ_{40}, S_{i0}, λ_{11}, λ_{21}, λ_{31}, λ_{41}, λ_{51}, λ_{61}, m_{s1}, m_{l1}, m_{i1}, m_{v1}, m_{w1}, m_{c1}, κ_{11}, κ_{21}, κ_{31}, κ_{41}, S_{10}, θ and n are given in Table 2.

TABLE 2. Constants of the model parameters.

λ_{10}	λ_{20}	λ_{30}	λ_{40}	λ_{50}	λ_{60}	m_{s0}	m_{l0}	m_{i0}	m_{v0}	m_{w0}	m_{c0}	κ_{10}	κ_{20}
0.8	0.7	2	0.5	1	0.2	0.8	4	2	0.5	1	0.2	0.8	1

κ_{30}	κ_{40}	S_{i0}	λ_{11}	λ_{21}	λ_{31}	λ_{41}	λ_{51}	λ_{61}	κ_{11}	κ_{21}	κ_{31}	κ_{41}	θ	n
0.8	10	10	0.8	0.7	2	0.5	1	0.2	0.8	0.2	0.8	4	2	0.2

m_{s1}	m_{l1}	m_{i1}	m_{v1}	m_{w1}	m_{c1}	S_{i1}	f_4^{max}	f_5^{max}	f_6^{max}	ζ_4	ζ_5	ζ_6
0.2	0.8	4	2	0.5	1	0.2	0.31	0.32	0.33	2	2.1	2.2

The first set of tests concerns the case of constant parameters. The second set of examples concerns the case of only T-periodic variable contact rates: $\lambda_1(t), \lambda_2(t)$, $\lambda_3(t)$, $\lambda_4(t)$, $\lambda_5(t)$, and $\lambda_6(t)$. The third set of examples illustrates a scenario where each model parameter is a periodic function.

3.1. **Fixed parameters.** Firstly, we examine the scenario in which all parameters are presumed to be constant. The model (2.1) takes the following form

$$\begin{cases} \dot{I}_l(t) = [\lambda_{10}f_1(V(t)) + \lambda_{20}f_2(I_l(t)) + \lambda_{30}f_3(I_p(t))]S(t) - (\kappa_{10}+m_{l0})I_l(t), \\ \dot{I}_p(t) = \kappa_{10}I_l(t) - m_{i0}(t)I_p(t) - \lambda_{40}f_4(I_p(t))T_l(t), \\ \dot{V}(t) = \kappa_{20}I_p(t) - m_{v0}V(t) - \lambda_{50}f_5(V(t))W(t), \\ \dot{S}(t) = m_{s0}S_{i0} - m_{s0}S(t) - [\lambda_{10}f_1(V(t)) + \lambda_{20}f_2(I_l(t)) + \lambda_{30}f_3(I_p(t))]S(t), \\ \dot{W}(t) = \kappa_{30}V(t) - m_{w0}W(t), \\ \dot{T}_l(t) = \kappa_{40}I_p(t) - m_{c0}T_l(t) - \lambda_{60}f_6(I_p(t))T_l(t). \end{cases} \tag{3.2}$$

Let us denote by $\mathcal{R}_0$, the basic reproduction number, that it is calculated when applying the next-generation matrix method [45,46]. Let

$$\mathbf{P} = \begin{pmatrix} \lambda_{20} f_2'(0) S_{i0} & \lambda_{30} f_3'(0) S_{i0} & \lambda_{10} f_1'(0) S_{i0} \\ 0 & 0 & 0 \\ 0 & 0 & 0 \end{pmatrix}, \quad \mathbf{\Lambda} = \begin{pmatrix} \kappa_{10} + m_{l0} & 0 & 0 \\ -\kappa_{10} & m_{i0} & 0 \\ 0 & -\kappa_{20} & m_{v0} \end{pmatrix},$$

and then

$$\mathbf{\Lambda^{-1}} = \begin{pmatrix} \dfrac{1}{\kappa_{10} + m_{l0}} & 0 & 0 \\ \dfrac{\kappa_{10}}{m_{i0}(\kappa_{10} + m_{l0})} & \dfrac{1}{m_{i0}} & 0 \\ \dfrac{\kappa_{10}\kappa_{20}}{m_{i0} m_{v0}(\kappa_{10} + m_{l0})} & \dfrac{\kappa_{20}}{m_{i0} m_{v0}} & \dfrac{1}{m_{v0}} \end{pmatrix}.$$

Therefore, the next-generation matrix, $\mathbf{P\Lambda^{-1}}$, is given by $\mathbf{P\Lambda^{-1}} = \mathbf{S_{i0}} \begin{pmatrix} a_1 & a_2 & a_3 \\ 0 & 0 & 0 \\ 0 & 0 & 0 \end{pmatrix}$ with

$a_1 = \dfrac{\kappa_{10}\kappa_{20}\lambda_{10} f_1'(0) + m_{i0} m_{v0} \lambda_{20} f_2'(0) + \kappa_{10} m_{v0} \lambda_{30} f_3'(0)}{m_{i0} m_{v0}(\kappa_{10} + m_{l0})}$, $a_2 = \dfrac{\kappa_{20}\lambda_{10} f_1'(0) + m_{v0}\lambda_{30} f_3'(0)}{m_{i0} m_{v0}}$,

and $a_3 = \dfrac{\lambda_{10} f_1'(0)}{m_{v0}}$. Therefore, $\mathcal{R}_0$ is given by

$$\mathcal{R}_0 = S_{i0} \frac{\kappa_{10}\kappa_{20}\lambda_{10} f_1'(0) + m_{i0} m_{v0} \lambda_{20} f_2'(0) + \kappa_{10} m_{v0} \lambda_{30} f_3'(0)}{m_{i0} m_{v0}(\kappa_{10} + m_{l0})}.$$

We provide several examples validating the theoretical findings concerning the behavior of the trajectories of model (3.2). In Figure 1, we consider a set of parameters $f_1^{max} = 0.15, f_2^{max} = 0.25, f_3^{max} = 0.35$, $f_4^{max} = 0.31$, $f_5^{max} = 0.32$ and $f_6^{max} = 0.33$, $\zeta_1 = 11, \zeta_2 = 9$, and $\zeta_3 = 13$ $\zeta_4 = 2$, $\zeta_5 = 2.1$ and $\zeta_6 = 2.2$ such that $\mathcal{R}_0 \approx 0.8 < 1$. The trajectory converges to $Q_0 = (0, 0, 0, S_{i0}, 0, 0)$ where Q_0 represents the *HIV*-free equilibrium point . The trajectories for several initial values converge to the same *HIV*-free equilibrium point is shown in Figure 2. In Figure 3, we provide the trajectories where $f_1^{max} = 0.25$, $f_2^{max} = 0.35$, $f_3^{max} = 0.45$, $f_4^{max} = 0.31$, $f_5^{max} = 0.32$ and $f_6^{max} = 0.33$ $\zeta_1 = 1.5$, $\zeta_2 = 1.2$, and $\zeta_3 = 1.3$ $\zeta_4 = 2$, $\zeta_5 = 2.1$ and $\zeta_6 = 2.2$ such that $\mathcal{R}_0 \approx 9.68 > 1$. The trajectory converges to the endemic equilibrium point. In Figure 4, we provide the trajectories for several initial values that converge to the same endemic equilibrium point.

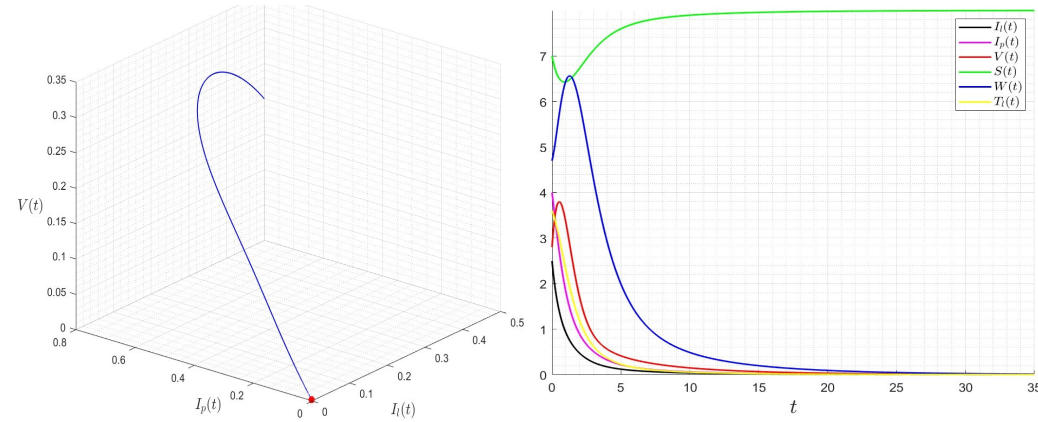

Figure 1. Dynamics of (3.2) with initial condition $(I_l^0, I_p^0, V^0, S^0, W^0, T_l^0) = (2.5, 4, 2.8, 7, 4.7, 3.6) \in \mathbb{R}_+^6$ for $f_1^{max} = 0.15$, $f_2^{max} = 0.25$, $f_3^{max} = 0.35$, $f_4^{max} = 0.31$, $f_5^{max} = 0.32$ and $f_6^{max} = 0.33$, $\zeta_1 = 11$, $\zeta_2 = 9$, $\zeta_3 = 13$, $\zeta_4 = 2$, $\zeta_5 = 2.1$ and $\zeta_6 = 2.2$ then $\mathcal{R}_0 \approx 0.8 < 1$.

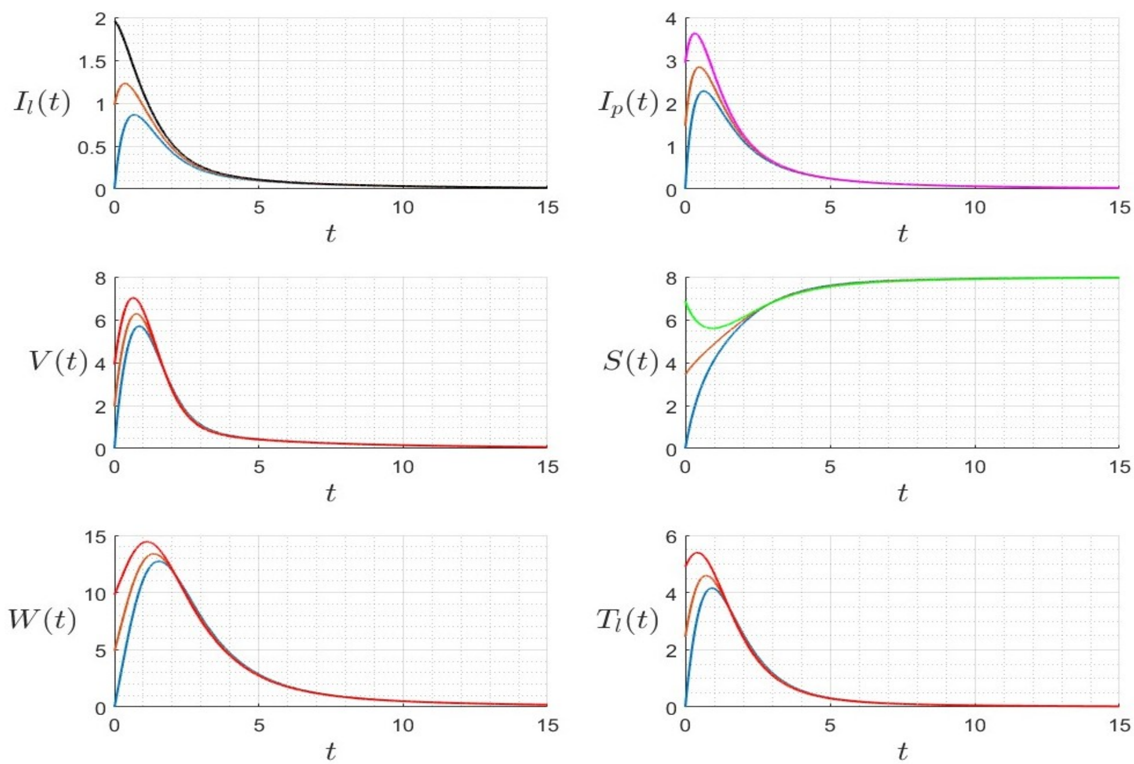

Figure 2. Trajectories dynamics for several initial conditions (different colors) where $f_1^{max} = 0.15$, $f_2^{max} = 0.25$, $f_3^{max} = 0.35$, $f_4^{max} = 0.31$, $f_5^{max} = 0.32$ and $f_6^{max} = 0.33$, $\zeta_1 = 11$, $\zeta_2 = 9$, $\zeta_3 = 13$, $\zeta_4 = 2$, $\zeta_5 = 2.1$ and $\zeta_6 = 2.2$, ($\mathcal{R}_0 \approx 0.8 < 1$).

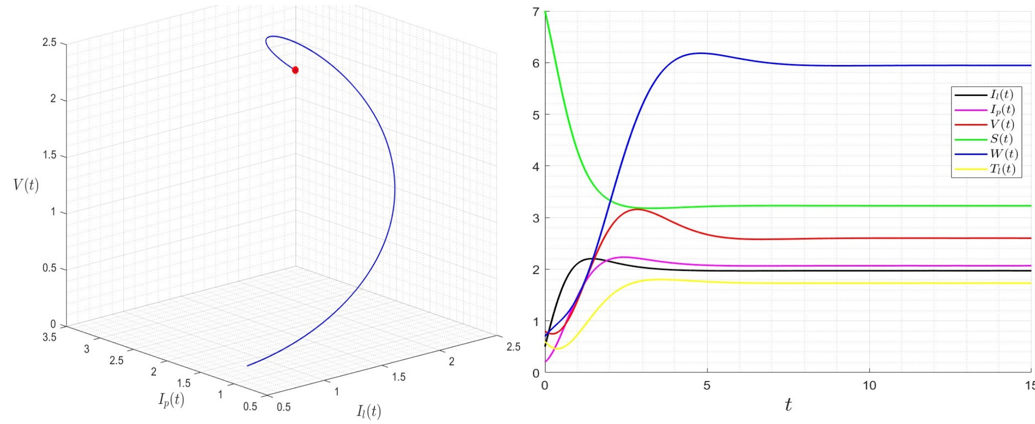

Figure 3. Dynamics of (3.2) with initial condition $(I_l^0, I_p^0, V^0, S^0, W^0, T_l^0) = (0.5, 0.2, 0.8, 7, 0.7, 0.6) \in \mathbb{R}_+^6$ for $f_1^{max} = 0.25$, $f_2^{max} = 0.35$, $f_3^{max} = 0.45$, $f_4^{max} = 0.31$, $f_5^{max} = 0.32$ and $f_6^{max} = 0.33$,$\zeta_1 = 1.5$, $\zeta_2 = 1.2$, and $\zeta_3 = 1.3$, $\zeta_4 = 2$, $\zeta_5 = 2.1$ and $\zeta_6 = 2.2$ then $\mathcal{R}_0 \approx 9.68 > 1$.

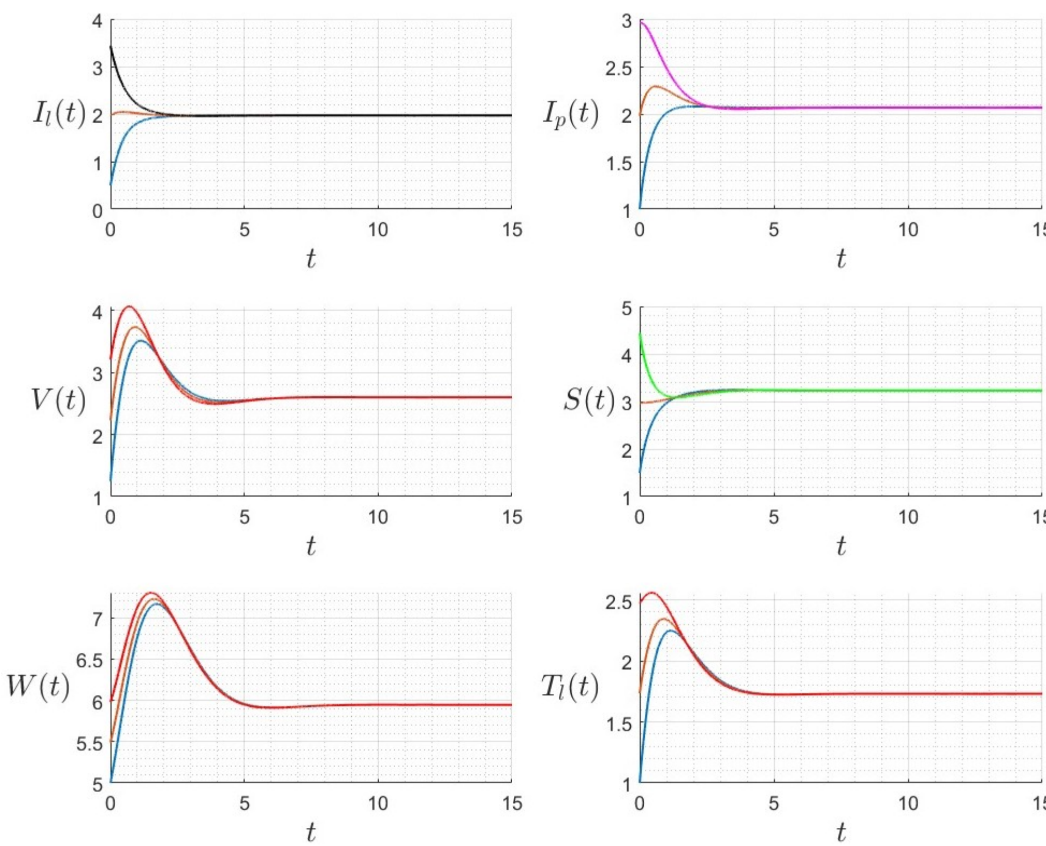

Figure 4. Trajectories dynamics for several initial conditions (different colors) where $f_1^{max} = 0.25$, $f_2^{max} = 0.35$, $f_3^{max} = 0.45$, $f_4^{max} = 0.31$, $f_5^{max} = 0.32$ and $f_6^{max} = 0.33$,$\zeta_1 = 1.5$, $\zeta_2 = 1.2$, and $\zeta_3 = 1.3$, $\zeta_4 = 2$, $\zeta_5 = 2.1$ and $\zeta_6 = 2.2$ ($\mathcal{R}_0 \approx 9.68 > 1$).

3.2. **Periodic transmission rates.** In this step, we conduct numerical simulations on model (2.1), utilizing a linear function to express the transmission rate. Only the seasonally forced T-periodic functions $\lambda_1(t), \lambda_2(t), \lambda_3(t), \lambda_4(t)$, and $\lambda_6(t)$ are time-dependent. The dynamics take the following form:

$$\begin{cases} \dot{I}_l(t) = [\lambda_1(t)f_1(V(t)) + \lambda_2(t)f_2(I_l(t)) + \lambda_3(t)f_3(I_p(t))]S(t) - (\kappa_{10} + m_{l0})I_l(t), \\ \dot{I}_p(t) = \kappa_{10}I_l(t) - m_{i0}(t)I_p(t) - \lambda_4(t)f_4(I_p(t))T_l(t), \\ \dot{V}(t) = \kappa_{20}I_p(t) - m_{v0}V(t) - \lambda_5(t)f_5(V(t))W(t), \\ \dot{S}(t) = m_{s0}S_{i0} - m_{s0}S(t) - [\lambda_1(t)f_1(V(t)) + \lambda_2(t)f_2(I_l(t)) + \lambda_3(t)f_3(I_p(t))]S(t), \\ \dot{W}(t) = \kappa_{30}V(t) - m_{w0}W(t), \\ \dot{T}_l(t) = \kappa_{30}I_p(t) - m_{c0}T_l(t) - \lambda_6(t)f_6(I_p(t))T_l(t). \end{cases} \tag{3.3}$$

The approximation of $\mathcal{R}_0$ is performed using the time-averaged system. We provide several examples validating the theoretical findings concerning the behavior of the trajectories of model (3.3). Considering a set of parameters $f_1^{max} = 0.15$, $f_2^{max} = 0.25$, $f_3^{max} = 0.35$, $f_4^{max} = 0.31$, $f_5^{max} = 0.32$ and $f_6^{max} = 0.33$ $\zeta_1 = 11$, $\zeta_2 = 9$, and $\zeta_3 = 13$ $\zeta_4 = 2$, $\zeta_5 = 2.1$ and $\zeta_6 = 2.2$ such that $\mathcal{R}_0 \approx 0.8 < 1$. The trajectory converges to $Q_0 = (0, 0, 0, S_{i0}, 0, 0)$ as shown in Figure 5 . In Figure 6, we provide the trajectories for several initial values that converge to the same *HIV*-free equilibrium point. In Figure 7, we provide the trajectories where $f_1^{max} = 0.25$, $f_2^{max} = 0.35$, $f_3^{max} = 0.45$, $f_4^{max} = 0.31$, $f_5^{max} = 0.32$ and $f_6^{max} = 0.33$, $\zeta_1 = 1.5$, $\zeta_2 = 1.2$, and $\zeta_3 = 1.3$ $\zeta_4 = 2$, $\zeta_5 = 2.1$ and $\zeta_6 = 2.2$ such that $\mathcal{R}_0 \approx 9.68 > 1$. The trajectory converges to the periodic trajectory expressing the persistence of *HIV*. Provide the trajectories for several initial values that converge to the same periodic trajectory indicated in Figure 8.

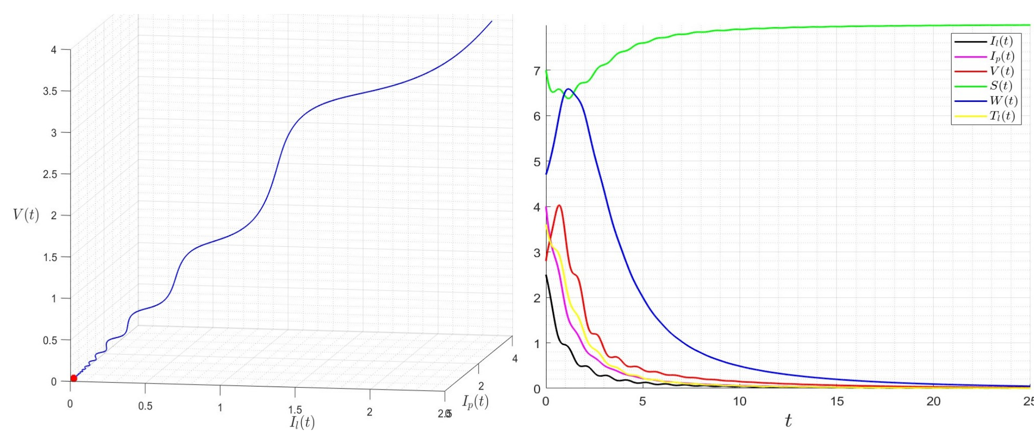

FIGURE 5. Dynamics of (3.3) with initial condition $(I_l^0, I_p^0, V^0, S^0, W^0, T_l^0) = (2.5, 4, 2.8, 7, 4.7, 3.6) \in \mathbb{R}_+^6$ for $f_1^{max} = 0.15$, $f_2^{max} = 0.25$, $f_3^{max} = 0.35$, $\zeta_1 = 11$, $\zeta_2 = 9$, and $\zeta_3 = 13$ then $\mathcal{R}_0 \approx 0.8 < 1$.

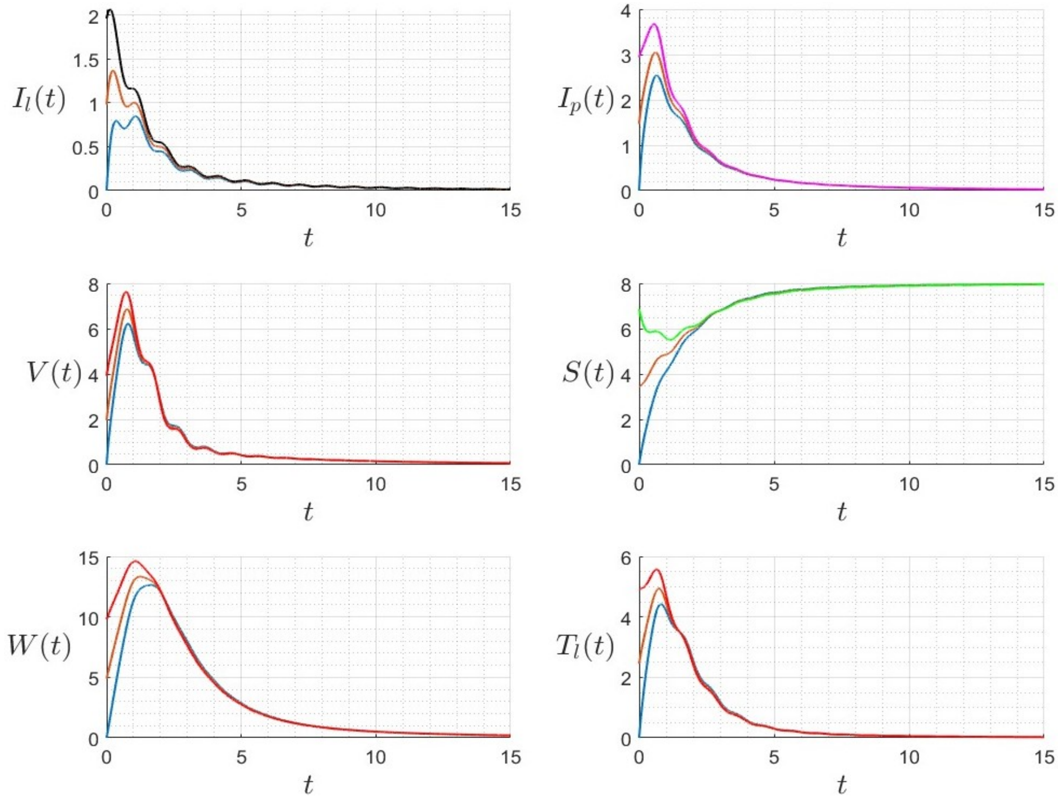

Figure 6. Trajectories dynamics for several initial conditions (different colors) where $f_1^{max} = 0.15$, $f_2^{max} = 0.25$, $f_3^{max} = 0.35$, $\zeta_1 = 11$, $\zeta_2 = 9$, and $\zeta_3 = 13$ ($\mathcal{R}_0 \approx 0.8 < 1$).

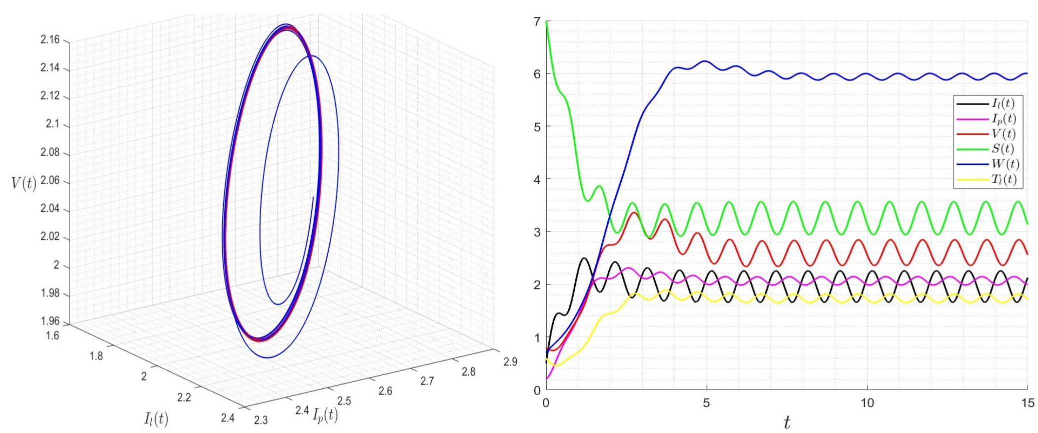

Figure 7. Dynamics of (3.3) with initial condition $(I_l^0, I_p^0, V^0, S^0, W^0, T_l^0) = (0.5, 0.2, 0.8, 7, 0.7, 0.6) \in \mathbb{R}_+^6$ for $f_1^{max} = 0.25$, $f_2^{max} = 0.35$, $f_3^{max} = 0.45$, $f_4^{max} = 0.31$, $f_5^{max} = 0.32$ and $f_6^{max} = 0.33$,$\zeta_1 = 1.5$, $\zeta_2 = 1.2$, and $\zeta_3 = 1.3$, $\zeta_4 = 2$, $\zeta_5 = 2.1$ and $\zeta_6 = 2.2$ then $\mathcal{R}_0 \approx 9.68 > 1$.

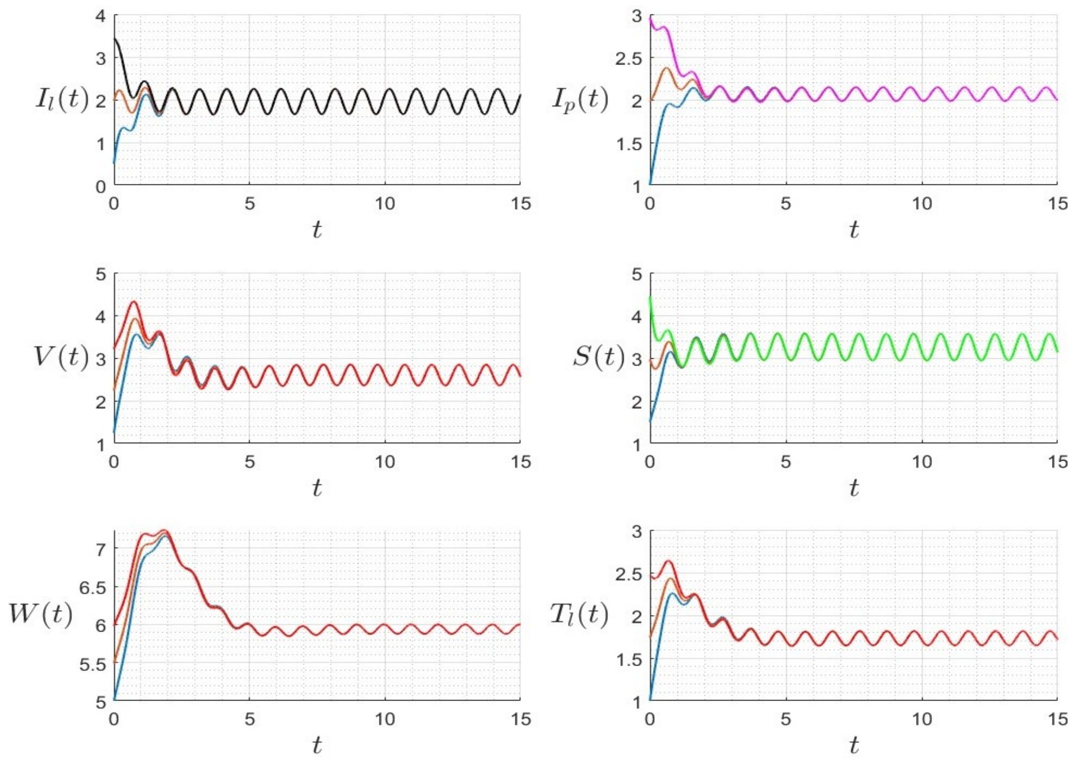

FIGURE 8. Trajectories dynamics for several initial conditions (different colors) where $f_1^{max} = 0.25$, $f_2^{max} = 0.35$, $f_3^{max} = 0.45$, $f_4^{max} = 0.31$, $f_5^{max} = 0.32$ and $f_6^{max} = 0.33$,$\zeta_1 = 1.5$, $\zeta_2 = 1.2$, and $\zeta_3 = 1.3$, $\zeta_4 = 2$, $\zeta_5 = 2.1$ and $\zeta_6 = 2.2$ ($\mathcal{R}_0 \approx 9.68 > 1$).

3.3. **Full periodic environment.** In the final scenario, let's pretend that the model is this shape by assuming that all of the parameters are periodic functions that reflect a completely periodic environment:

$$\begin{cases} \dot{I}_l(t) = [\lambda_1(t)f_1(V(t)) + \lambda_2(t)f_2(I_l(t)) + \lambda_3(t)f_3(I_p(t))]f(S(t)) - (\kappa_1(t) + m_l(t))I_l(t), \\ \dot{I}_p(t) = \kappa_1(t)I_l(t) - m_p(t)I_p(t) - \lambda_4(t)f_4(I_p(t))T_l(t), \\ \dot{V}(t) = \kappa_2(t)I_p(t) - m_v(t)V(t) - \lambda_5(t)f_5(V(t))W(t), \\ \dot{S}(t) = m_s(t)S_i(t) - m_s(t)S(t) - [\lambda_1(t)f_1(V(t)) + \lambda_2(t)f_2(I_l(t)) + \lambda_3(t)f_3(I_p(t))]S(t), \\ \dot{W}(t) = \kappa_3(t)V(t) - m_w(t)W(t), \\ \dot{T}_l(t) = \kappa_4(t)I_p(t) - m_c(t)T_l(t) - \lambda_6(t)f_6(I_p(t))T_l(t). \end{cases} \tag{3.4}$$

Again, the approximation of $\mathcal{R}_0$ is performed using the time-averaged system. We provide several examples validating the theoretical findings concerning the behaviour of the trajectories of model (3.4). In Figure 9, we consider a set of parameters $f_1^{max} = 0.15$, $f_2^{max} = 0.25$, $f_3^{max} = 0.35$, $f_4^{max} = 0.31$, $f_5^{max} = 0.32$ and $f_6^{max} = 0.33$ $\zeta_1 = 11$, $\zeta_2 = 9$, and $\zeta_3 = 13$ $\zeta_4 = 2$, $\zeta_5 = 2.1$ and $\zeta_6 = 2.2$ such that $\mathcal{R}_0 \approx 0.8 < 1$. The trajectory converges to the *HIV*-free periodic solution $\mathcal{Q}_0(t) = (0, 0, 0, S*(t), 0, 0)$. In Figure 10, we provide the trajectories for several initial values which converge to the same *HIV*-free periodic solution. In Figure 11, we provide the trajectories where $f_1^{max} = 0.25$, $f_2^{max} = 0.35$,

$f_3^{max} = 0.45$, $f_4^{max} = 0.31$, $f_5^{max} = 0.32$ and $f_6^{max} = 0.33$ $\zeta_1 = 1.5$, $\zeta_2 = 1.2$, and $\zeta_3 = 1.3$ $\zeta_4 = 2$, $\zeta_5 = 2.1$ and $\zeta_6 = 2.2$ such that $\mathcal{R}_0 \approx 9.68 > 1$. The trajectory converges to the periodic trajectory expressing the persistence of *HIV*. Figure 12 illustrates the trajectories for various initial values that ultimately converge to the same periodic trajectory.

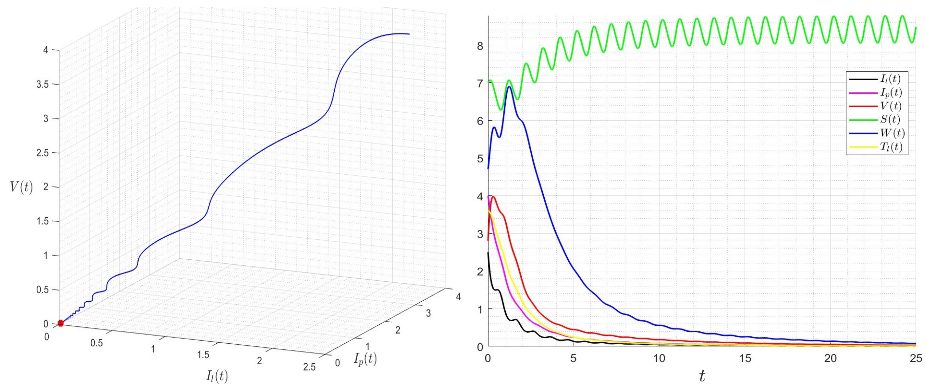

FIGURE 9. Dynamics of (3.4) with initial condition $(I_l^0, I_p^0, V^0, S^0, W^0, T_l^0) = (2.5, 4, 2.8, 7, 4.7, 3.6) \in \mathbb{R}_+^6$ for $f_1^{max} = 0.15$, $f_2^{max} = 0.25$, $f_3^{max} = 0.35$, $f_4^{max} = 0.31$, $f_5^{max} = 0.32$ and $f_6^{max} = 0.33$, $\zeta_1 = 11$, $\zeta_2 = 9$, $\zeta_3 = 13$, $\zeta_4 = 2$, $\zeta_5 = 2.1$ and $\zeta_6 = 2.2$, then $\mathcal{R}_0 \approx 0.8 < 1$.

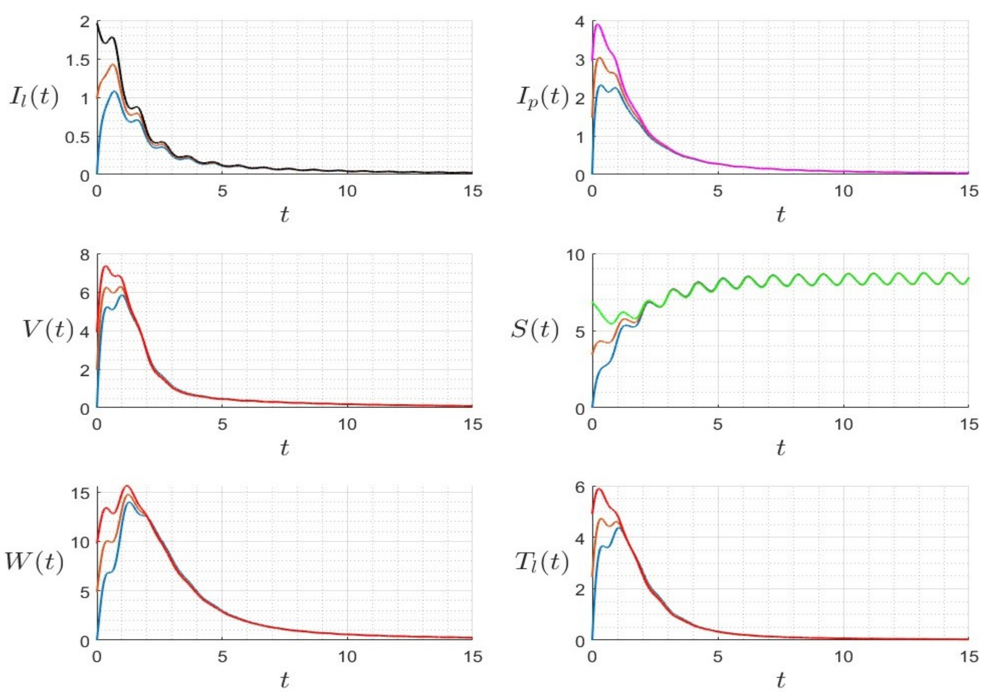

FIGURE 10. Trajectories dynamics for several initial conditions (different colors) where $f_1^{max} = 0.15$, $f_2^{max} = 0.25$, $f_3^{max} = 0.35$, $f_4^{max} = 0.31$, $f_5^{max} = 0.32$ and $f_6^{max} = 0.33$, $\zeta_1 = 11$, $\zeta_2 = 9$, $\zeta_3 = 13$, $\zeta_4 = 2$, $\zeta_5 = 2.1$ and $\zeta_6 = 2.2$, ($\mathcal{R}_0 \approx 0.8 < 1$).

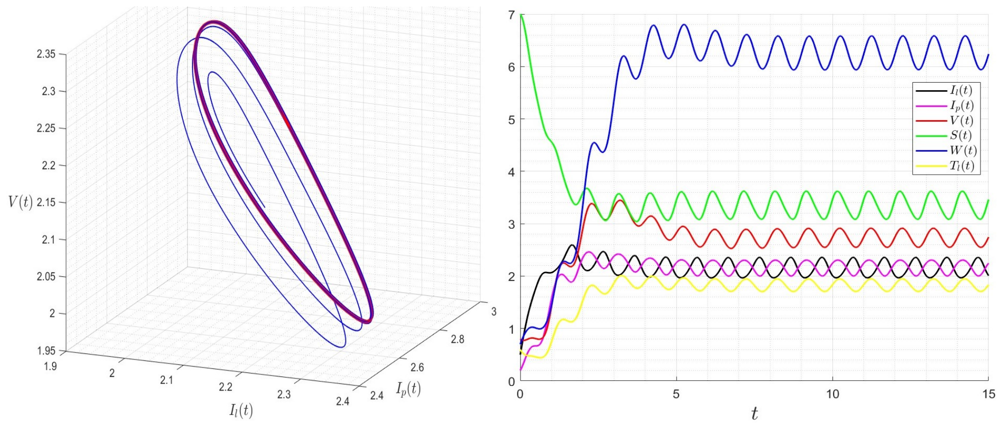

Figure 11. Dynamics of (3.4) with initial condition $(I_l^0, I_p^0, V^0, S^0, W^0, T_l^0) = (0.5, 0.2, 0.8, 7, 0.7, 0.6) \in \mathbb{R}_+^6$ for $f_1^{max} = 0.25$, $f_2^{max} = 0.35$, $f_3^{max} = 0.45$, $f_4^{max} = 0.31$, $f_5^{max} = 0.32$ and $f_6^{max} = 0.33$,$\zeta_1 = 1.5$, $\zeta_2 = 1.2$, and $\zeta_3 = 1.3$, $\zeta_4 = 2$, $\zeta_5 = 2.1$ and $\zeta_6 = 2.2$ then $\mathcal{R}_0 \approx 9.68 > 1$.

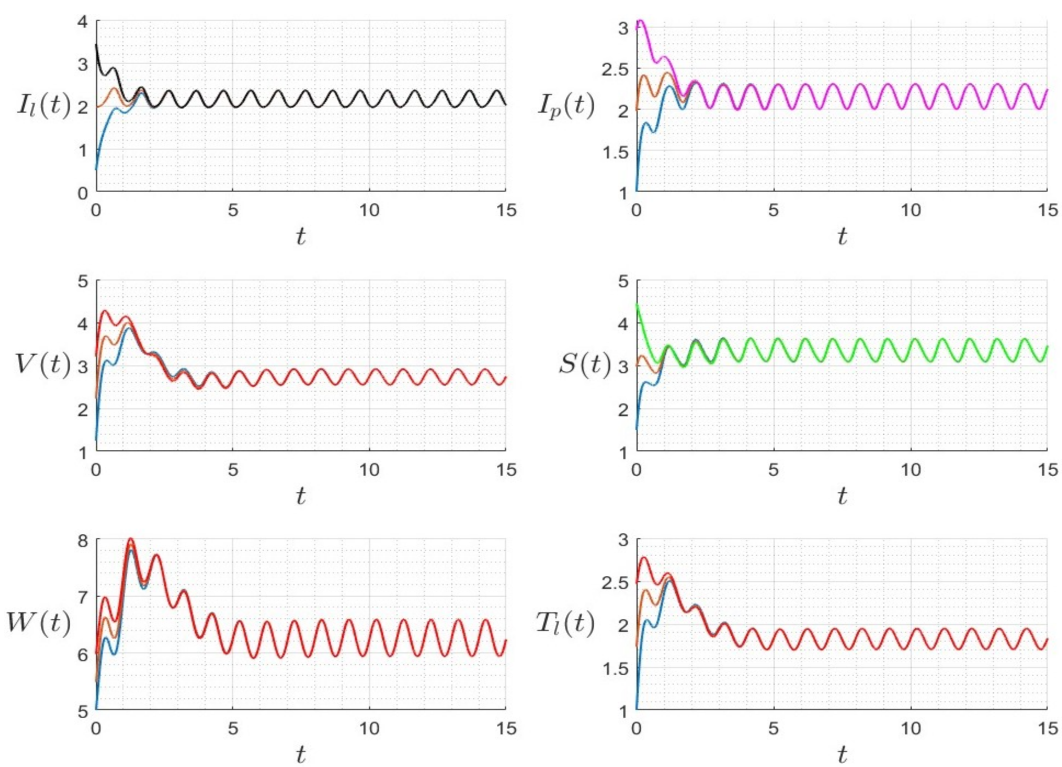

Figure 12. Trajectories dynamics for several initial conditions (different colors) where $f_1^{max} = 0.25$, $f_2^{max} = 0.35$, $f_3^{max} = 0.45$, $f_4^{max} = 0.31$, $f_5^{max} = 0.32$ and $f_6^{max} = 0.33$,$\zeta_1 = 1.5$, $\zeta_2 = 1.2$, and $\zeta_3 = 1.3$, $\zeta_4 = 2$, $\zeta_5 = 2.1$ and $\zeta_6 = 2.2$ ($\mathcal{R}_0 \approx 9.68 > 1$).

4. Conclusions

The *HIV* dynamical system proposed in [41] was extended to a model with general transmission and neutralization rates by considering a new compartment describing the B cell variation in a periodic environment. The dynamics deal with three routes of infection, taking into account infection from both latently infected cells and productively infected cells. General nonlinear nonnegative increasing functions give both the incidence rates of infection and the neutralization rates of infected cells and viruses. The basic infection reproduction number was defined through the spectral radius of an integral operator. We have established the model's asymptotic stability analysis concerning the value of the basic reproduction number to unity. We have performed numerical examples using specific forms of Holling's type II functions, covering all incidence and neutralization rates. We performed numerical simulations for three scenarios to confirm the results, showing that the solution converges to a limit cycle.

Conflicts of Interest: The authors declare that there are no conflicts of interest regarding the publication of this paper.

References

[1] N.C. Grassly, C. Fraser, Mathematical Models of Infectious Disease Transmission, Nat. Rev. Microbiol. 6 (2008), 477–487. https://doi.org/10.1038/nrmicro1845.

[2] F. Brauer, C. Castillo-Chavez, A. Mubayi, S. Towers, Some Models for Epidemics of Vector-Transmitted Diseases, Infect. Dis. Model. 1 (2016), 79–87. https://doi.org/10.1016/j.idm.2016.08.001.

[3] A. Sisk, N. Fefferman, A Network Theoretic Method for the Basic Reproductive Number for Infectious Diseases, Methods Ecol. Evol. 13 (2022), 2503–2515. https://doi.org/10.1111/2041-210X.13978.

[4] H.W. Hethcote, The Mathematics of Infectious Diseases, SIAM Rev. 42 (2000), 599–653. https://doi.org/10.1137/S0036144500371907.

[5] R.M. Anderson, R.M. May, Population Biology of Infectious Diseases: Part I, Nature 280 (1979), 361–367. https://doi.org/10.1038/280361a0.

[6] T.W. Chun, D. Finzi, J. Margolick, K. Chadwick, D. Schwartz, R.F. Siliciano, In Vivo Fate of HIV-1-Infected T Cells: Quantitative Analysis of the Transition to Stable Latency, Nat. Med. 1 (1995), 1284–1290. https://doi.org/10.1038/nm1295-1284.

[7] F. Sallusto, D. Lenig, R. Förster, M. Lipp, A. Lanzavecchia, Two Subsets of Memory T Lymphocytes with Distinct Homing Potentials and Effector Functions, Nature 401 (1999), 708–712. https://doi.org/10.1038/44385.

[8] L. Gattinoni, E. Lugli, Y. Ji, et al. A Human Memory T Cell Subset with Stem Cell–like Properties, Nat. Med. 17 (2011), 1290–1297. https://doi.org/10.1038/nm.2446.

[9] H. Abbey, An Examination of the Reed-Frost Theory of Epidemics, Human Biol. 24 (1952), 201.

[10] F. Kermack, D. McKendrick, A Contribution to the Mathematical Theory of Epidemics, Proc. R. Soc. Lond. Ser. A, 115 (1927), 700–721. https://doi.org/10.1098/rspa.1927.0118.

[11] W.H. Hamer, M. Cantab, F. Lond, The Milroy Lectures on Epidemic Disease in England–the Evidence of Variability and of Persistency of Type, The Lancet 167 (1906), 569–574. https://doi.org/10.1016/S0140-6736(01)80187-2.

[12] D.J. Daley, J. Gani, Epidemic Modelling: An Introduction, Cambridge University Press, 1999. https://doi.org/10.1017/CBO9780511608834.

[13] A.M. Elaiw, N.A. Almuallem, A. Hobiny, Effect of RTI Drug Efficacy on the HIV Dynamics with Two Cocirculating Target Cells, J. Comput. Anal. Appl. 23 (2017), 209–228.

[14] A.M. Elaiw, N.A. Almuallem, Global Dynamics of Delay-distributed HIV Infection Models with Differential Drug Efficacy in Cocirculating Target Cells, Math. Methods Appl. Sci. 39 (2016), 4–31. https://doi.org/10.1002/mma.3453.

[15] A. Elaiw, Nada. Almuallem, X. Wang, Global Analysis of an Extended HIV Dynamics Model with General Incidence Rate, J. Biol. Syst. 23 (2015), 401–421. https://doi.org/10.1142/S0218339015500217.

[16] A.M. Elaiw, N.A. Almuallem, Global Properties of Delayed-HIV Dynamics Models with Differential Drug Efficacy in Cocirculating Target Cells, Appl. Math. Comput. 265 (2015), 1067–1089. https://doi.org/10.1016/j.amc.2015.06.011.

[17] A.M. Elaiw, N.A. Almuallem, Global Properties for HIV Dynamics Models with Differential Drug Efficacy in Cocirculating Target Cells, J. Comput. Theor. Nanosci. 12 (2015), 3506–3515. https://doi.org/10.1166/jctn.2015.4231.

[18] S. Alsahafi, S. Woodcock, Exploring HIV Dynamics and an Optimal Control Strategy, Mathematics 10 (2022), 749. https://doi.org/10.3390/math10050749.

[19] M.E. Hajji, A.H. Albargi, et al. A Mathematical Investigation of an "SVEIR" Epidemic Model for the Measles Transmission, Math. Biosci. Eng. 19 (2022), 2853–2875. https://doi.org/10.3934/mbe.2022131.

[20] M. El Hajji, D.M. Alshaikh, N.A. Almuallem, Periodic Behaviour of an Epidemic in a Seasonal Environment with Vaccination, Mathematics 11 (2023), 2350. https://doi.org/10.3390/math11102350.

[21] A. Alshehri, M. El Hajji, Mathematical Study for Zika Virus Transmission with General Incidence Rate, AIMS Math. 7 (2022), 7117–7142. https://doi.org/10.3934/math.2022397.

[22] M.E. Hajji, M.F.S. Aloufi, M.H. Alharbi, Influence of Seasonality on Zika Virus Transmission, AIMS Math. 9 (2024), 19361–19384. https://doi.org/10.3934/math.2024943.

[23] M.A. Nowak, C.R.M. Bangham, Population Dynamics of Immune Responses to Persistent Viruses, Science 272 (1996), 74–79. https://doi.org/10.1126/science.272.5258.74.

[24] A.S. Perelson, A.U. Neumann, M. Markowitz, J.M. Leonard, D.D. Ho, HIV-1 Dynamics in Vivo: Virion Clearance Rate, Infected Cell Life-Span, and Viral Generation Time, Science 271 (1996), 1582–1586. https://doi.org/10.1126/science.271.5255.1582.

[25] M.A. Nowak, S. Bonhoeffer, G.M. Shaw, R.M. May, Anti-Viral Drug Treatment: Dynamics of Resistance in Free Virus and Infected Cell Populations, J. Theor. Biol. 184 (1997), 203–217. https://doi.org/10.1006/jtbi.1996.0307.

[26] A.S. Perelson, P. Essunger, Y. Cao, et al. Decay Characteristics of HIV-1-Infected Compartments during Combination Therapy, Nature 387 (1997), 188–191. https://doi.org/10.1038/387188a0.

[27] R.J. De Boer, A.S. Perelson, Target Cell Limited and Immune Control Models of HIV Infection: A Comparison, J. Theor. Biol. 190 (1998), 201–214. https://doi.org/10.1006/jtbi.1997.0548.

[28] D. Wodarz, A.L. Lloyd, V.A.A. Jansen, M.A. Nowak, Dynamics of Macrophage and T Cell Infection by HIV, J. Theor. Biol. 196 (1999), 101–113. https://doi.org/10.1006/jtbi.1998.0816.

[29] S. Bajaria, Predicting Differential Responses to Structured Treatment Interruptions during HAART, Bull. Math. Biol. 66 (2004), 1093–1118. https://doi.org/10.1016/j.bulm.2003.11.003.

[30] M. El Hajji, R.M. Alnjrani, Periodic Trajectories for HIV Dynamics in a Seasonal Environment With a General Incidence Rate, Int. J. Anal. Appl. 21 (2023), 96. https://doi.org/10.28924/2291-8639-21-2023-96.

[31] M. El Hajji, Periodic Solutions for Chikungunya Virus Dynamics in a Seasonal Environment with a General Incidence Rate, AIMS Math. 8 (2023), 24888–24913. https://doi.org/10.3934/math.20231269.

[32] M. El Hajji, Periodic Solutions for an "SVIQR" Epidemic Model in a Seasonal Environment with General Incidence Rate, Int. J. Biomath. (2024), 2450033. https://doi.org/10.1142/S1793524524500335.

[33] B.S. Alshammari, D.S. Mashat, F.O. Mallawi, Mathematical and Numerical Investigations for a Cholera Dynamics With a Seasonal Environment, Int. J. Anal. Appl. 21 (2023), 127. https://doi.org/10.28924/2291-8639-21-2023-127.

[34] H. Almuashi, Mathematical Analysis for the Influence of Seasonality on Chikungunya Virus Dynamics, Int. J. Anal. Appl. 22 (2024), 86. https://doi.org/10.28924/2291-8639-22-2024-86.

[35] F.A. Al Najim, Mathematical Analysis for a Zika Virus Dynamics in a Seasonal Environment, Int. J. Anal. Appl. 22 (2024), 71. https://doi.org/10.28924/2291-8639-22-2024-71.

[36] W. Wang, X.Q. Zhao, Threshold Dynamics for Compartmental Epidemic Models in Periodic Environments, J. Dyn. Differ. Equ. 20 (2008), 699–717. https://doi.org/10.1007/s10884-008-9111-8.

[37] Y. Nakata, T. Kuniya, Global Dynamics of a Class of SEIRS Epidemic Models in a Periodic Environment, J. Math. Anal. Appl. 363 (2010), 230–237. https://doi.org/10.1016/j.jmaa.2009.08.027.

[38] M. El Hajji, N.S. Alharbi, M.H. Alharbi, Mathematical Modeling for a CHIKV Transmission Under the Influence of Periodic Environment, Int. J. Anal. Appl. 22 (2024), 6. https://doi.org/10.28924/2291-8639-22-2024-6.

[39] M. El Hajji, F.A.S. Alzahrani, R. Mdimagh, Impact of Infection on Honeybee Population Dynamics in a Seasonal Environment, Int. J. Anal. Appl. 22 (2024), 75. https://doi.org/10.28924/2291-8639-22-2024-75.

[40] M. El Hajji, F.A.S. Alzahrani, M.H. Alharbi, Mathematical Analysis for Honeybee Dynamics Under the Influence of Seasonality, Mathematics 12 (2024), 3496. https://doi.org/10.3390/math12223496.

[41] M. El Hajji, R.M. Alnjrani, Periodic Behaviour of HIV Dynamics with Three Infection Routes, Mathematics 12 (2023), 123. https://doi.org/10.3390/math12010123.

[42] G. Frobenius, Uber Matrizen aus Nicht Negativen Elementen, Sitzungsberichte Preussische Akademie der Wissenschaft, Berlin, (1912). https://doi.org/10.3931/e-rara-18865.

[43] F. Zhang, X.Q. Zhao, A Periodic Epidemic Model in a Patchy Environment, J. Math. Anal. Appl. 325 (2007), 496–516. https://doi.org/10.1016/j.jmaa.2006.01.085.

[44] X.Q. Zhao, Dynamical Systems in Population Biology, Springer, New York, (2003).

[45] O. Diekmann, J.A.P. Heesterbeek, J.A.J. Metz, On the Definition and the Computation of the Basic Reproduction Ratio $\mathcal{R}_0$ in Models for Infectious Diseases in Heterogeneous Populations, J. Math. Biol. 28 (1990), 365–382. https://doi.org/10.1007/BF00178324.

[46] P. Van Den Driessche, J. Watmough, Reproduction Numbers and Sub-Threshold Endemic Equilibria for Compartmental Models of Disease Transmission, Math. Biosci. 180 (2002), 29–48. https://doi.org/10.1016/S0025-5564(02)00108-6.